International Journal of Dynamics and Control (2022) 10:2124–2138
https://doi.org/10.1007/s40435-022-00940-6

Direct synthesis-based fractional-order PID controller design: application to AVR system

Nadir Fergani[1]

Received: 19 December 2021 / Revised: 3 March 2022 / Accepted: 8 March 2022 / Published online: 9 April 2022

Abstract
In this paper, a novel method for tuning $PI^{\lambda}D^{\mu}$ controllers is proposed. Based on the direct synthesis approach, the proposed technique consists of taking the closed-loop system equivalent to Bode's ideal loop transfer function. Using a semi-analytical technique, the parameters of the controller are derived from the desired closed-loop transfer function and the plant's input/output signals without using any identification technique. Simulation examples are given to show the efficiency and the applicability of the proposed method to high-order and time delay systems. The results confirm that the proposed controller satisfies the dynamics requirements with iso-damping property when compared with two other related tuning methods. As an application example, the proposed tuning method is applied to the automatic voltage regulator system in order to study the efficiency and robustness of the proposed controller.

Keywords Fractional-order PID controller design · Bode's ideal loop transfer function · Direct synthesis approach · Analytical tuning · Automatic voltage regulator

1 Introduction

Nowadays, the fractional-order control, which is the use of the aspect of the non-integer-order derivative or integral operators in controller design, became a very important strategy in the control system field. Indeed, the first sign of fractional-order control existence was introduced by Bode in [1] where he proposed the fractional-order integrator as an ideal loop transfer function. The main reason of this choice is that it gives a closed-loop system that is insensitive to gain changes [2]. This idea gave the starting point to Oustaloup in 1991 [3] where he proposed the CRONE control as the first application of the fractional-order control. Since 1999, when Podlubny has proposed the $PI^{\lambda}D^{\mu}$ [4], which is a generalization of classical PID controller, most of the developments in the fractional-order controller tuning methods were based on his work. These tuning methods are classified into three main categories according to review presented in [5] namely numerical, analytical and rule-based methods. However, due to the higher number of parameters of the fractional PID compared to the classical PID controller, the tuning of its parameters remains always a challenging task demonstrated by the recent proposed methods in the literature [6–19].

In classical control, the PID controller is the most commonly used for industrial applications. In fact, the success of this controller is due to its simplicity and achievability to solve the most required performance specifications in control systems. However, the tuning of this controller remains an interest topic of research to the present day. In this context, the two popular approaches namely internal model control IMC [20] and direct synthesis DS [21] have known a wide acceptance in the research community in the field of PID design, this success may be justified by their simplicity and their explicit tuning formulas, allowing the derivation of the controller analytically by using the plant's model. In addition, the controller obtained by these approaches has not necessarily a PID form, but the choice of an appropriate desired closed-loop transfer function helps the designer to derivate a PID structure [21].

Since the fractional-order control is considered as an extension of classical control, most of the theories of integer-order systems and controllers were extended to the fractional ones. The IMC has been extended to the fractional-order PID controller design in [11, 13], where a new controller structure that includes a fractional filter has been proposed

✉ Nadir Fergani
nadirfergani@yahoo.fr; n.fergani@crti.dz

[1] Research Center in Industrial Technologies CRTI, P.O. Box 64, Cheraga, Algiers, Algeria

in [13]. On the other hand, the second approach; which is the DS-based technique, has not yet been extended to the case of $PI^{\lambda}D^{\mu}$ controller design. In this paper, a novel DS-based tuning method of fractional PID is proposed, inspired from the recent tuning technique of the classical PID controller proposed in [22]. This method consists of making the closed-loop system equivalent to the Bode's ideal loop transfer function. The tuning formula is a semi-analytical and data-based technique where a set of the closed-loop system input/output signals allows the designer to extract the five parameters of the $PI^{\lambda}D^{\mu}$ controller without the need for any model approximation of the plant. The main advantage of this tuning method is that the closed-loop system behaves as the desired system in the selected frequency band which allows manipulating the dynamics of controlled system by adjusting the desired one. The basic idea of the tuning algorithm is presented and illustrative examples are presented to test the effectiveness and the robustness of the fractional PID controller tuned by the proposed approach.

Many industrial processes are modeled by transfer functions with delay; this physical phenomenon makes the control of this type very difficult, especially when the system is characterized by a long time delay. Indeed, the presence of time delay θ in the open loop gives a phase equal to $-\omega\theta$, the phase angle decreases monotonically with frequency, with this slope in the open-loop phase we cannot obtain a flat phase [2].

In the literature, different approaches are used for controlling time delay systems. In the case of the desired system, this last usually includes the same time delay as the one in the plant [23, 24]. In this variant, the designer looses the iso-damping property. The second approach consists of using a well-known Smith predictor as in the works [25–27], two degrees of freedom (2-DOF) fractional-order internal model controller was proposed in [28] and direct synthesis-based controller was proposed in [29]. The third approach is based on satisfying the condition that the derivative argument of open-loop transfer functions to be zero at unity gain crossover frequency. This condition verifies that the phase of open loop to be constant around gain crossover frequency which gives the iso-damping property for the closed-loop system [30]. Many existing tuning methods have used this condition in controller design [6–10]. An exception in [14] the designer has used a loop shaping method and solved the problem with numerical optimization. In the present work, the Bode's ideal transfer function as desired system is used, the results presented in this paper show that the open-loop system with the $PI^{\lambda}D^{\mu}$ controller may have the same behavior of the desired system for a given frequency band although the presence of time delay in the plant.

Knowing that the fractional control has been proven successful for application in power generation system as in [31, 32], an application of the proposed controller design methodology to an automatic voltage regulator (AVR) is carried out. Results show implementation simplicity and efficiency of the controlled system when using the proposed controller.

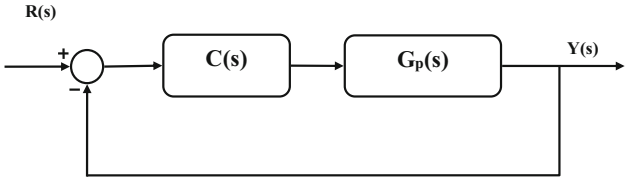

Fig. 1 Classical unity feedback control

2 Direct synthesis-based control design

Let us consider a feedback control system shown in Fig. 1 with $G_{\mathrm{p}}(s)$ as the plant's transfer function; the closed-loop transfer function is given by:

$$G_{\mathrm{cl}}(s) = \frac{C(s)G_{\mathrm{p}}(s)}{1 + C(s)G_{\mathrm{p}}(s)} \tag{1}$$

The controller transfer function can be derived from Eq. (1) as:

$$C(s) = \frac{G_{cl}(s)}{G_p(s)(1 - G_{cl}(s))} \tag{2}$$

When replacing the closed-loop transfer function by the desired transfer function G_{cl_d} with the assumption that $G_p(s)$ is known, the desired controller is given by:

$$C(s) = \frac{G_{cl\_d}(s)}{G_p(s)(1 - G_{cl\_d}(s))} \tag{3}$$

In the general case, the controller obtained when using the DS approach has not necessarily the PI or PID form. Nevertheless, by choosing an appropriate desired closed-loop function, the PID structure can be derived as in [21], where the author proposes an analytical design for some known models such as first and second order plus time delay and integrator plus time delay.

The advantage of using the DS approach is that the optimal controller is well-known and the performance of the closed-loop system is manipulated by adjusting the desired model. However, this technique, as the IMC technique, depends on the plant's model which is generally not available in many industrial applications. This issue has been treated in [22], where the designer formulated the same DS approach by tuning the PI/PID controller analytically using process data without any model approximation of the process. In the next section, we present a projection of this new tuning method

for the design of fractional-order PID controller where an appropriate desired closed-loop system is considered and the controller design is carried out for a set-point change instead of load disturbance rejection as in the work [22]. The objective of selecting the set-point change as the control goal is to achieving the iso-damping property in the closed-loop system.

3 Direct synthesis-based PI$^{\lambda}$D$^{\mu}$ tuning

3.1 Proposed controller design

PI$^{\lambda}$D$^{\mu}$ controller is the most common structure of fractional control which is an extension of the classical PID controller. This controller includes the three actions proportional, integral and derivative with additional flexibility compared to the classical one. This flexibility is due to its two additional parameters λ and μ which can improve the performance and robustness of the feedback control system.

The transfer function of PI$^{\lambda}$D$^{\mu}$ controller is given by:

$$C(s) = k_c + \frac{T_i}{s^{\lambda}} + T_d s^{\mu} \tag{4}$$

where λ and μ are the order of integrator and derivative actions, respectively, these two parameters are generally chosen real in the range 0 to 2 [5].

For DS-based approach, the optimal controller is given by Eq. (3), so we have:

$$C(s) = k_c + \frac{T_i}{s^{\lambda}} + T_d s^{\mu} = \frac{G_{cl\_d}(s)}{G_p(s)(1 - G_{cl\_d}(s))} \tag{5}$$

where the desired closed-loop transfer function is chosen as follows:

$$G_{cl\_d}(s) = \frac{1}{1 + \left(\frac{s}{\omega_c}\right)^m} \tag{6}$$

This system, called Bode's ideal transfer function, is widely used as reference model in control system design [2]. The main advantage of this system is that it has the iso-damping property which is a very suitable property for the controlled system. The two positive real parameters m and ω_c must be chosen in a way that the desired closed-loop system satisfies the desired performances. If the dynamics requirements are given in terms of unity gain crossover frequency and phase margin so the two parameters m and ω_c are given by:

- ω_c is unity gain crossover frequency.
- $m = 2(1\text{-}\varphi_m/\pi)$ (φ_m is the phase margin).

The transfer function H(s) is given by:

$$H(s) = \frac{G_{cl\_d}(s)}{G_p(s)(1 - G_{cl\_d}(s))} = \frac{U(s)\, G_{cl\_d}(s)}{Y(s)\,(1 - G_{cl\_d}(s))} \tag{7}$$

where $U(s)$ and $Y(s)$ are the Laplace transform of the plant's input and output signals, respectively. So, from Eqs. (5) and (7) we have:

$$k_c + T_i s^{-\lambda} + T_d s^{\mu} = H(s) \tag{8}$$

This equation can be rewritten as:

$$\begin{bmatrix} \frac{1}{H(s)} & \frac{s^{-\lambda}}{H(s)} & \frac{s^{\mu}}{H(s)} \end{bmatrix} p = 1 \tag{9}$$

where $p = \begin{bmatrix} p_1 & p_2 & p_3 \end{bmatrix}^T$ and $\begin{cases} p_1 = k_c \\ p_2 = T_i \\ p_3 = T_d \end{cases}$.

Equation (9) is expressed in the frequency domain by substituting $s = j\omega$ as follows:

$$\begin{bmatrix} \frac{1}{H(j\omega)} & \frac{(j\omega)^{-\lambda}}{H(j\omega)} & \frac{(j\omega)^{\mu}}{H(j\omega)} \end{bmatrix} p = 1 \tag{10}$$

Initially, we consider that the parameters λ and μ are known. So, the unknown parameters vector $\boldsymbol{p}$ can be calculated in the way that Eq. (10) is satisfied in the entire frequency range $[\omega_{\min}\ \omega_{\max}]$. Thus, Eq. (10) is rewritten as:

$$1_n - \psi\ p = 0 \tag{11}$$

where $\psi = \begin{bmatrix} \psi_1 \\ \psi_2 \\ \vdots \\ \psi_n \end{bmatrix}, \psi_i = \begin{bmatrix} \frac{1}{H(j\omega_i)} & \frac{(j\omega_i)^{-\lambda}}{H(j\omega_i)} & \frac{(j\omega_i)^{\mu}}{H(j\omega_i)} \end{bmatrix}$.

$\boldsymbol{1_n}$ denotes an $n \times 1$ column vector of ones.

Since the plant's dynamic performance is depending essentially on unity gain crossover frequency, the frequency range $[\omega_{\min}\ \omega_{\max}]$ is chosen around this frequency ω_c.

When we use the classical PID, the ψ matrix is known as in the work presented in [22], where the three parameters are derived analytically. It's not the case with the PI$^{\lambda}$D$^{\mu}$ where the ψ matrix depends on the two parameters λ and μ. The exponent positions of these last make very difficult their separation from the ψ matrix in Eq. (11). As it is known that the values of λ and μ are usually in the range of 0 to 2, we can numerically scan these two parameters from 0 to 2 and derivate analytically the $\boldsymbol{p}$ vector for each value of λ and μ. Hence, the best values of λ and μ are those that satisfy the optimization criterion that assured more likely Eq. (11).

The resolution of Eq. (11) is formulated as in [22] where the author proposed to solve a weighted least-squares problem:

$$\min_{p} \left(\phi - \tilde{\psi}\ \mathrm{p}\right)^{\mathrm{T}} \tilde{W} \left(\phi - \tilde{\psi}\ p\right) \tag{12}$$

With

$$\phi = \begin{bmatrix} 1_n \\ 0_n \end{bmatrix} \quad ; \quad \tilde{\psi} = \begin{bmatrix} \mathrm{Re}(\psi) \\ \mathrm{Im}(\psi) \end{bmatrix}; \quad \tilde{W} = \begin{bmatrix} W & 0 \\ 0 & W \end{bmatrix}$$

$\boldsymbol{0_n}$ is an $n \times 1$ column vector of zeros;

$\mathrm{Re}(\psi)$ and $\mathrm{Im}(\psi)$ denote real and imaginary parts of the complex matrix ψ. and $\boldsymbol{W}$ is a weighting matrix. An appropriate choice of W for stable process is:

$$W = diag\left[\frac{1}{\omega_1}\ \frac{1}{\omega_2}\ \ldots\ \frac{1}{\omega_n}\right] \tag{13}$$

This choice gives a priority to high frequencies over low frequencies in the optimization problem (12).

The analytical solution of weighted least-squares problem (12) is given by:

$$p = \left(\tilde{\psi}^T \tilde{W} \tilde{\psi}\right)^{-1} \tilde{\psi}^T \tilde{W} \phi \tag{14}$$

Once the vector $\boldsymbol{p}$ is calculated, the five parameters of the $\mathrm{PI}^{\lambda}\mathrm{D}^{\mu}$ controller are obtained. The tuning algorithm is detailed as follows:

Tuning algorithm:

For: *λ=0 to λ=2 with sampling of 0.01*

For: *μ=0 to μ=2 with sampling of 0.01*

- *Calculate the matrix ψ (λ,μ).*
- *Obtain parameters vector* ***p*** *from eq. (14).*
- *Calculate criterion function from eq. (13).*

End

End

- *Select the optimum parameters which are minimizing the function give by eq. (15).*

END

This resolution technique is chosen because of its simplicity and the fact that it has an analytical solution allowing the design of the controller without using the optimization techniques.

The optimization criterion used in this work is a function of two variables λ and μ is given by:

$$F(\lambda, \mu) = \left(\phi - \tilde{\psi}\ p\right)^{\mathrm{T}} \tilde{W} \left(\phi - \tilde{\psi}\ p\right) \tag{15}$$

This criterion is chosen in order to satisfy more likely Eq. (11).

Since the three parameters k_c, T_i and T_d are analytically obtained from Eq. (14) and the two additional parameters λ and μ are numerically computed by scanning their range, the proposed solution is called a semi-analytical technique.

3.2 Fourier transform of the input/output signals

In the previous subsection, the controller parameters p are given analytically function of ˜ψ matrix using Eq. (14), where ˜ψ is function of $H(j\omega_i)$ according to (11). Numerical computation of $H(j\omega_i)$ for all frequencies ω_i can be done by using Eq. (7) where $H(j\omega_i)$ is function of the Fourier transform of the input/output signals $U(j\omega_i)$ and $Y(j\omega_i)$. Finally, the controller tuning can be done through the time domain signals $u(t)$ and $y(t)$ without need of the plant's model. In this section, we use the technique presented in [22]. The input and output signals are, respectively, decomposed as follows:

$$\begin{aligned} u(t) &= \Delta u(t) + u_s \\ y(t) &= \Delta y(t) + y_s \end{aligned} \tag{16}$$

Here, $\Delta u(t)$ and u_s are the transit and final steady-state values of $u(t)$, respectively. The same for the output signal $y(t)$. It is known that $\Delta u(t)$ and $\Delta y(t)$ are approximately zero in steady state, so their Fourier transforms are given by:

$$\begin{aligned} \Delta U(j\omega_i) &= \int_0^{\infty} \Delta u(t) e^{-j\omega_i t} \mathrm{d}t \approx \int_0^{\mathrm{T}} \Delta u(t) e^{-j\omega_i t} \mathrm{d}t \\ \Delta Y(j\omega_i) &= \int_0^{\infty} \Delta y(t) e^{-j\omega_i t} \mathrm{d}t \approx \int_0^{\mathrm{T}} \Delta y(t) e^{-j\omega_i t} \mathrm{d}t \end{aligned} \tag{17}$$

where T is the acquisition time of input and output signals, its value must be greater than the settling time of the plant. So, Eq. (17) can be calculated at each frequency ω_i by numerical integration or by the FFT technique. Finally, the Fourier transform of the input–output signals is given by:

$$\begin{aligned} U(j\omega_i) &= \Delta U(j\omega_i) + \frac{u_s}{j\omega_i} \\ Y(j\omega_i) &= \Delta Y(j\omega_i) + \frac{y_s}{j\omega_i} \end{aligned} \tag{18}$$

3.3 Simulation results

To exhibit the effectiveness of the proposed method and its online application, the closed-loop data $u(t)$ and $y(t)$ were generated by simulating a closed-loop system with an initial controller, then the tuning algorithm is applied. Two different examples are presented in this section, in the first example

a complete study is presented that includes the sensitivity to the noise measurements and the chosen initial tuning. In the second example, only time and frequency responses are presented.

The following examples show that the proposed tuning method is not influenced by the initial (existing) controller used to generate the closed-loop data.

3.3.1 Example 1: high-order systems

Let use the first example with the transfer function given by:

$$G_{\mathrm{p1}}(s) = \frac{1}{(1+s)^3} \tag{19}$$

The design specifications are given by:

$-\varphi_{\mathrm{m}} = 60$ deg.
$-\omega_{\mathrm{c}} = 0.3$ rad/s.

These specifications are satisfied by the desired fractional-order system:

$$G_{\mathrm{cl\_d}}(s) = \frac{1}{1+\left(\frac{s}{0.3}\right)^{1.33}} \tag{20}$$

We use the controller tuned by the analytical technique proposed in [24] using the following design specifications ($\varphi_{\mathrm{m}} = 60$ deg, $\omega_{\mathrm{c}} = 0.3$ rad/sec) which is given as follows:

$$C(s) = \frac{0.5926}{s^{0.0774}}\left(1 + \frac{0.4292}{s^{1.0648}}\right) \tag{21}$$

This controller is used for comparison and also to generate the first initial tuning closed-loop data.

For a second initial tuning, the flowing controller is used:

$$C(s) = (1 + \frac{1}{s} + s) \tag{22}$$

Figures 2 and 3 show the two closed-loop data used for proposed controller design.

Figure 4 shows the Bode plot of the plant transfer function (19) and those estimated from process data by calculating $Y(j\omega)/U(j\omega)$.

By using a frequency band [0.1 2] rad/sec with sampling 0.05 rad/s, we obtain the following controller:

$$C_{\mathrm{p}}(s) = 0.8517 + \frac{0.2763}{s^{1.24}} + 0.4454\ s^{1.302} \tag{23}$$

These five parameters give an optimum criterion F (1.24, 1.3) = 0.03412 as it is shown in Fig. 5. Note that the F function has a convex form which implies that it has one global optimum in the presented rage.

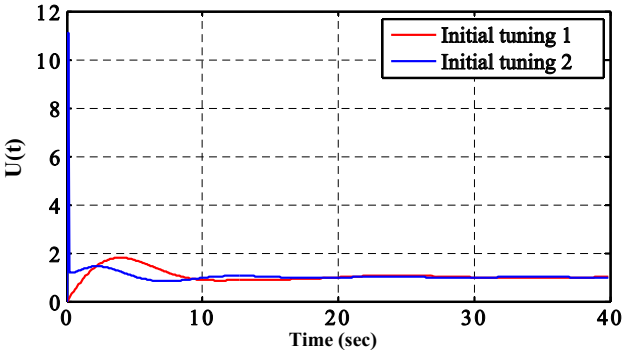

Fig. 2 Control law signals used for proposed controller design

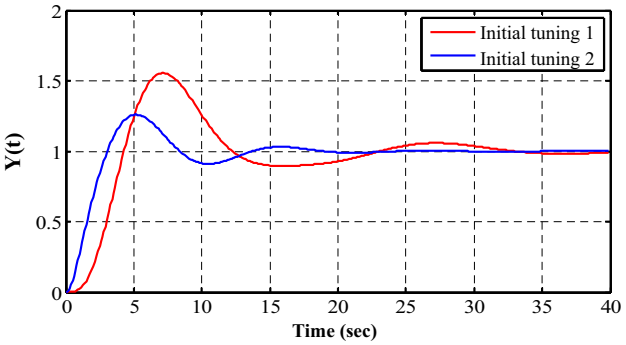

Fig. 3 Output signals used for proposed controller design

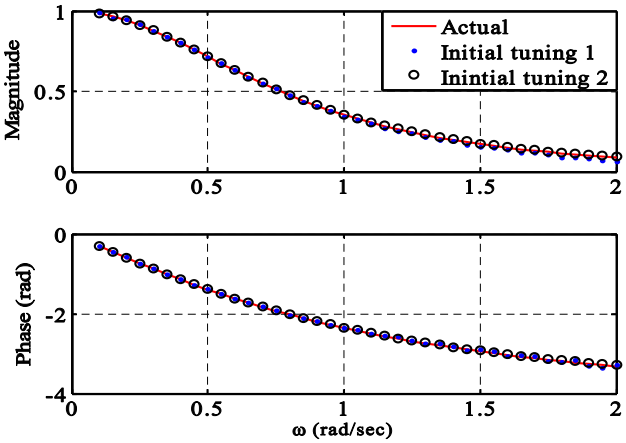

Fig. 4 Frequency response of the process and those estimated from process data

Figure 6 shows the Bode diagrams of the open-loop system with the controllers (21), (23) and the desired open system (20).

We can see that the phase is flat around $\omega_{\mathrm{c}} = 0.3$ rad/s which implies that the closed-loop system controlled with proposed controller is robust to gain variations. These results are shown in Fig. 7. On the other hand, the system controlled with (21) has not this property, as shown in Fig. 8, the main

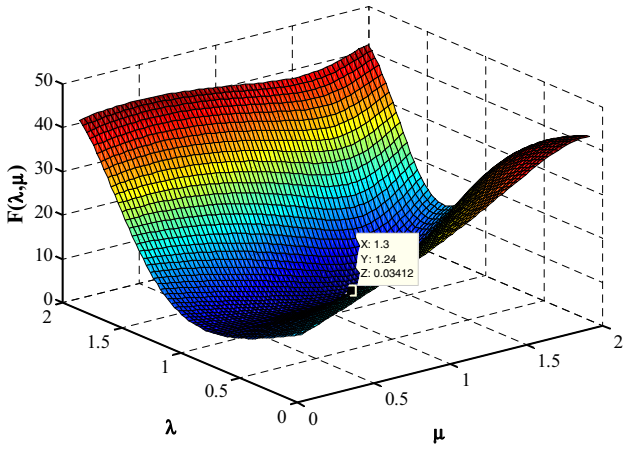

Fig. 5 Optimum criterion of Eq. (15) for the first example

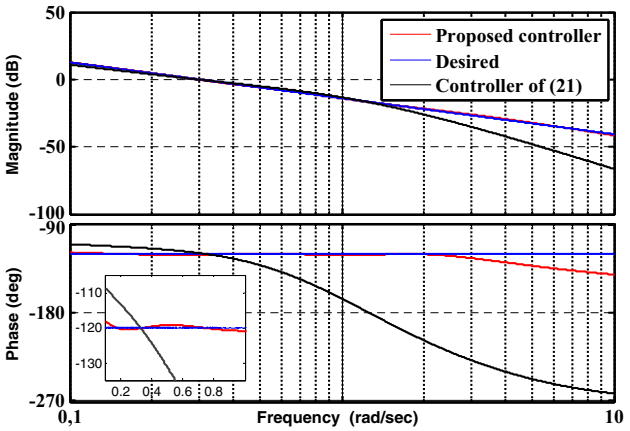

Fig. 6 Bode diagrams of the open-loop transfer functions

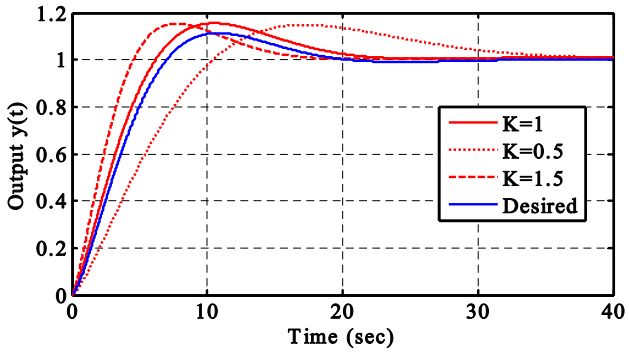

Fig. 7 Step responses of the closed-loop system G_{p1} with different gain values (using the proposed controller) red line and the desired response blue line

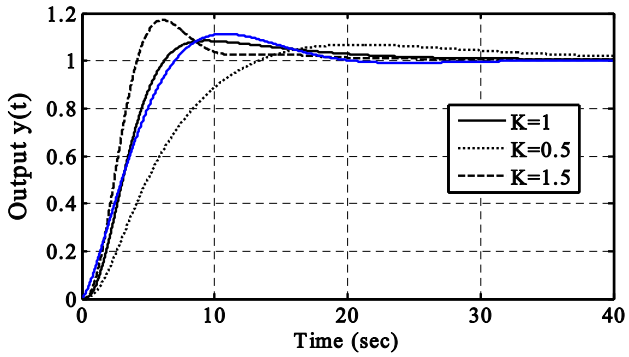

Fig. 8 Step responses of the closed-loop system G_{p1} with different gain values (using the controller given by (21)) black line and the desired response blue line

reason is that because the considered reference model in the method [24] is the Bode's ideal transfer function with time delay.

Table 1 shows the different characteristics of the closed-loop system compared with the controller (21) and the desired specifications where Mp is the overshoot, t_s is the settling time and M_s is the peak value of the sensitivity function.

Remark: From Figs. 7 and 8, the closed-loop response of the nominal plant with the proposed controller seems not better than that of (21) in terms of overshoot. Such result is obtained due to the weakness in design precision of the controller (21) compared to the proposed one. Table 1 shows that the proposed controller gives the closest performance to desired one.

In practice, data signals are noisy due to the sensors limitations and the effects of their power supply. To verify the applicability of the proposed tuning method, a Gaussian white noise with a standard deviation of 0.05 is added to input–output signals. Figure 9 shows the estimated frequency response obtained from noisy data of the second initial tuning. It's clear that the estimated frequency response obtained from the estimated data is approximately the same with the calculated one and the controller designed from noisy data is given by:

$$C_{pn}(s) = 0.8621 + \frac{0.2719}{s^{1.24}} + 0.4373\ s^{1.33} \tag{24}$$

Table 2 shows the obtained $PI^{\lambda}D^{\mu}$ parameters from different data used for the design where $C_{in1}(s)$ and $C_{in2}(s)$ are, respectively, the controllers obtained from first and second initial tuning. It is clear that no remarkable change is observed in the $PI^{\lambda}D^{\mu}$ parameters, which means that the proposed method is insensitive to the process data.

3.3.2 Example 2: time delay system

The transfer function of the plant is given as follows:

$$G_{p2}(s) = \frac{0.0015}{(s^2 + 0.1547\,s + 0.004357)} e^{-8s} \tag{25}$$

Table 1 Frequency and time domain characteristics

Controllers	φ_m (deg)	ω_c (rad/sec)	M_p (%)	t_s (s)	M
Reference closed-loop system	60	0.3	11.4	18.11	–
Controller (21)	61.6	0.297	8.1	22.76	1.39
The proposed controller	59.6	0.296	15.5	20.62	1.15

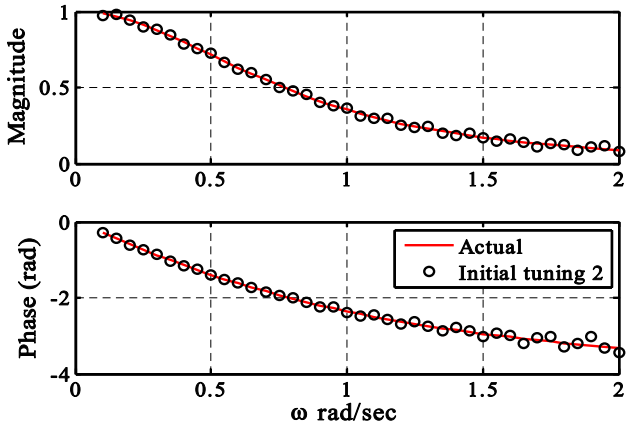

Fig. 9 Frequency response of the process and its estimate from noisy data

The design specifications are given by:

$-\varphi_m = 60$ deg.
$-\omega_c = .01$ rad/s

These specifications are satisfied by the desired fractional-order system:

$$G_{cl\_d}(s) = \frac{1}{1 + \left(\frac{s}{0.01}\right)^{1.33}} \tag{26}$$

By using a frequency band [0.001 0.2] rad/sec with sampling 0.001 rad/s, we obtain the following controller:

$$C_p(s) = \left(1.0423 + \frac{0.0116}{s^{1.207}} + 22.8742 s^{1.52}\right) \tag{27}$$

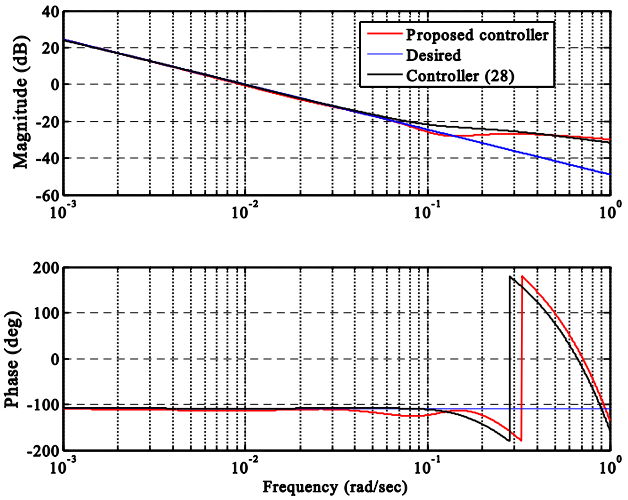

Fig. 10 Bode diagrams of the open-loop system with two controllers (27) and (28)

This controller is compared with the one proposed in [14], its transfer function is given by:

$$C(s) = \left(1.1030 + \frac{0.0141}{s^{1.1741}} + 18.1322 s^{1.2893}\right) \tag{28}$$

Figure 10 shows the frequency responses of the open-loop system controlled with (27) and (28) compared with desired system response. It is clear that the two open-loop systems satisfy the dynamics requirements and also have a flat phase around the gain crossover frequency $\omega_c = 0.01$ rad/s which gives a robustness property to the two controlled systems. This robustness to gain variations is shown in Fig. 11 where the two controllers satisfy the iso-damping property for a large band of gain variations. However, it is clear that the proposed controller is more robust than the controller proposed in [14] as it is shown

Table 2 Different controllers obtained from different process data

Parameters	C_p (s)	C_{in1} (s)	C_{in2} (s)	C_{pn} (s)
k_c	0.8517	0.8563	0.8518	0.8621
T_i	0.2763	0.2726	0.2723	0.2719
T_d	0.4454	0.4364	0.4379	0.4373
Λ	1.2310	1.2400	1.2400	1.2400
μ	1.3020	1.3000	1.3000	1.3300

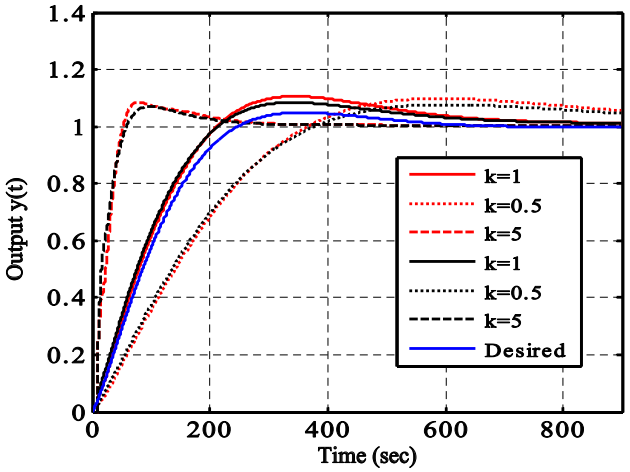

Fig. 11 Step responses of G_{p2} with different gain values using proposed controller (red line) and controller in (28) (black line) and the desired response (blue line)

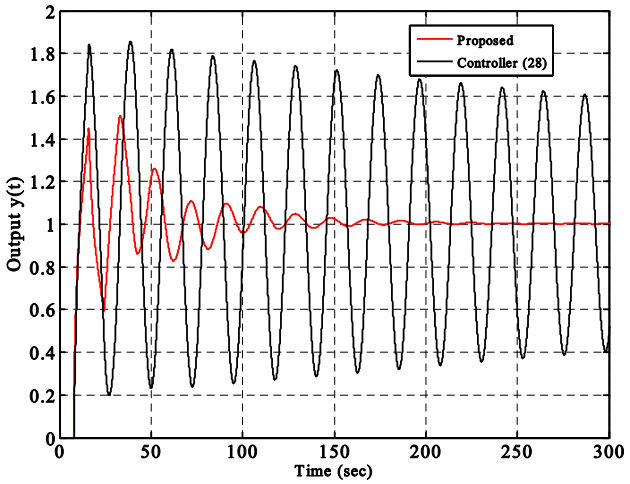

Fig. 12 Step responses of G_{p2} with the two controllers (27) and (28) with the plant static gain equals to 18

in Fig. 12 where the gain value equals 18; in addition, the proposed method is easily implemented and does not need the use of a complicated optimization algorithm as in [14].

From Fig. 11, we can easily see that the closed-loop system behaves as the desired system given by (26) despite the presence of time delay in the plant transfer function. This is the consequence of the overlapping between the open-loop and the desired system in the frequency range around the gain crossover frequency ω_c.

4 Fractional PID controller design for automatic voltage regulator system

In this section, the proposed tuning method is applied to tune the automatic voltage regulator (AVR) of a synchronous generator. The AVR has an important role in power generation systems where it grantees to maintain the output voltage of an alternator at a desired value in the presence of disturbance and load change. Figure 13 shows the block diagram of the AVR system.

The parameters of the AVR transfer functions components of are summarized in Table 3.

Most of existing research works in the literature as in [33–36] use the following parameters:

$T_a = 0.1$; $T_e = 0.4$; $T_g = 1$; $T_s = 0.01$; $k_a = 10$; $k_e = 1$; $k_g = 1$; $k_s = 1$; where the closed-loop system without controller is stable and the controller adjusts its performance. These parameters will be referred to as standard parameters in the following development.

In recent research work [37], authors use the parameters nominal values given by:

$T_a = 0.06$; $T_e = 0.7$; $T_g = 1.5$; $T_s = 0.0305$; $k_a = 25$; $k_e = 5.5$; $k_g = 0.85$; $k_s = 1$; where the closed loop without controller is unstable and it will be very difficult to optimize the controller using optimization algorithms.

Our study is divided into two parts:

- Design, with the proposed technique, a controller for standard parameters values and compare the closed-loop performances with those obtained in [33–36].
- Design a second controller for nominal parameters values and compare the closed-loop performances with those obtained in [37]. In this case, the plant's model is used instead of input/output signals.

In order to reduce the sensitivity to the noise measurement, the fractional-order derivative is implemented in series with a low pass filter given by 1/ (1 + 0.001 s).

Remark: As the AVR is a regulator and as the power generation systems always works in constant terminal voltage, the iso-damping property will not be taken into consideration for the $PI^{\lambda}D^{\mu}$ controller design. The same tuning algorithm will be used, except that the desired transfer function will be changed.

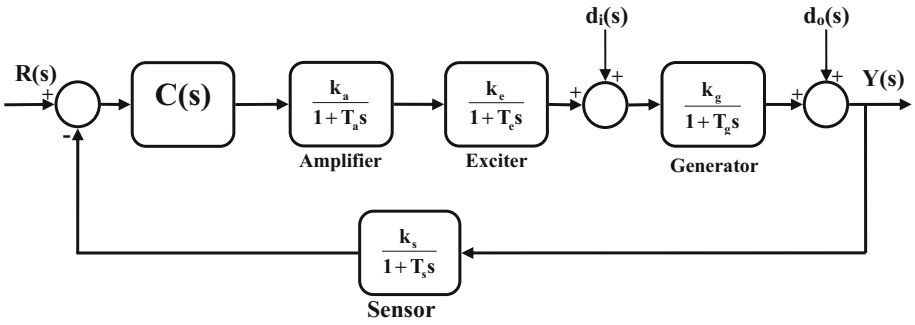

Fig. 13 Block diagram of AVR system

Table 3 AVR system's parameters

Component	Gain limit	Time constant limit
Amplifier	$10 \le k_a \le 40$	$0.02 \le T_a \le 0.1$
Exciter	$1 \le k_e \le 10$	$0.4 \le T_e \le 1$
Generator	$0.7 \le k_g \le 1$	$1 \le T_g \le 2$
Sensor	$k_s = 1$	$0.001 \le T_s \le 0.06$

4.1 Controller design for standard parameters values

The $PI^{\lambda}D^{\mu}$ controller, tuned by the proposed method, is designed for the AVR system of Fig. 13 where the plant's parameters are considered at its standard values and the closed-loop performance is compared with four different controllers proposed in [33–36].

As the AVR system is high-order system (fourth order), the proposed tuning method is applied using an appropriate desired closed-loop transfer function.

$$G_d(s) = \frac{1}{((0.02\,s)^2 + 2\,2.1\,0.02\,s\, + 1)^3}. \tag{29}$$

This high-order transfer function is proposed as reference model for the controlled system with reasonable parameters and control law signal.

By using the proposed tuning method with an initial tuning as the proportional gain equals to 1, the resulting proposed FOPID is shown in the first column of Table 4. This table summarizes the results of a comparative study of the proposed controller with two PID controllers [33–36] and two fractional PID controllers [35, 36] tuned using optimization techniques.

The closed-loop characteristics shown in Table 5 are divided into two parts:

- The first one shows the output step response characteristics: overshoot, rise time, settling time and the maximum of sensitivity function M_s.
- The second part gives the characteristics of the control signal in terms of maximum values $u_{\max}$, root mean square values u_{RMS} and total variation which is given by fowling equation:

$$TV = \sum_{k=0}^{\infty} |u(k+1) - u(k)|. \tag{30}$$

The steady-state error achieved by controllers is equal to zeros.

Figure (14) shows the time response of the AVR system controlled by the controllers given in Table 5. At $t = 0$ a 1^{pu} change in the reference $R(s)$ is applied in order to analyze the set-point tracking and at $t = 15$ a step unit change in the output disturbance is applied to analyze the disturbance rejection.

It is clear from Fig. 14 that the proposed controller achieves a reasonable time response compared with other controllers with two main advantages:

- The generation of a reasonable control law due to the choice of an appropriate desired closed-loop transfer function.
- Simple tuning procedure compared with other controllers based on optimization algorithms with different choices of fitness functions.

4.2 Controller designed for nominal values of system parameters

By using the nominal AVR system parameters:

4.2.1 $T_a = 0.06; T_e = 0.7; T_g = 1.5; T_s = 0.0305; k_a = 25; k_e = 5.5; k_g = 0.85; k_s = 1;$

The desired TF is given by:

$$G_d(s) = \frac{1}{(1 + 0.06\,\mathrm{s})^6}. \tag{31}$$

Table 4 Comparison of different controllers for AVR system

		Proposed controller	C_1 (s) [33]	C_2 (s) [35]	C_3 (s) [36]	C_4 (s) [34]
Controller parameters	K_c	0.4345	0.6198	2.4676	2.9944	0.9649
	T_i	0.4595	0.4165	0.3020	0.8165	0.610
	T_d	0.2531	0.2127	0.4230	0.5206	0.3110
	λ	0.9390	1	0.9700	1.1778	1
	μ	0.8630	1	1.3800	1.3647	1
Closed-Loop characteristics	M_p %	2.8846	**0.1167**	0.9182	6.8069	10.6639
		2.8846	8.7597	25.4738	34.366	10.3085
	t_r	0.2942	0.3050	0.0932	**0.0764**	0.1989
	t_s	**0.2942**	0.6117	0.3188	0.3039	0.4764
	M_s	1.3234	1.1746	3.6055	0.4120	0.9311
	u_{max}	**1.3234**	3.9198	2.1706	6.5863	3.7122
	u_{RMS}	1.4343	**1.3060**	1.3547	1.4405	1.4492
	TV	–	–	–	–	–
		10.1227	213.3098	8.7114 103	1.0467 104	311.9649
		10.1226	12.00	12.00	12.00	12.00
		0.2628	1.3636	48.0239	56.9760	1.9950
		0.2760	0.3078	0.7255	0.7621	0.3526
		32.2931	248.0053	1.0323 104	1.2233 104	364.8573
		32.2929	36.7921	103.5607	108.5495	37.8660

Remark: The closed-loop characteristics presented with two values for each index, first line without saturation and the second line with saturation in the control signal

Table 5 Comparison of the proposed controller with H_∞-based controller of [37]

	Case 1	Case 2	Case 3	Case 4	Case 5
Gain values					
k_a	25	40	40	10	10
k_e	5.5	10	10	1	1
k_g	0.85	1	1	0.7	0.7
k_s	1	1	1	1	1
Time constant					
T_a	0.06	0.1	0.02	0.02	0.1
T_e	0.7	1	0.4	0.4	1
T_g	1.5	2	1	1	2
T_s	0.0305	0.06	0.001	0.001	0.06
Proposed controller					
M_p%	**3.8604**	54.1431	21.35	0	**0**
t_s (2%)	**2.0669**	**3.3937**	1.3212	27.0567	19.162
Tv ($u(t)$)	**2.0810**	**2.3683**	**3.6517**	**2.9377**	**1.8337**
u_{RMS}	**0.0217**	**0.0237**	**0.0249**	**0.0832**	**0.0889**
H_∞ controller K (s)					
Mp%	15.0926	**41.7160**	**5.8828**	0	0.4929
t_s 2%	3.1006	3.8316	**0.5962**	**21.0872**	**13.7518**
Tv ($u(t)$)	4.6176	3.9997	13.1321	6.3814	4.1549
u_{RMS}	0.0300	0.0278	0.0568	0.0905	0.0952

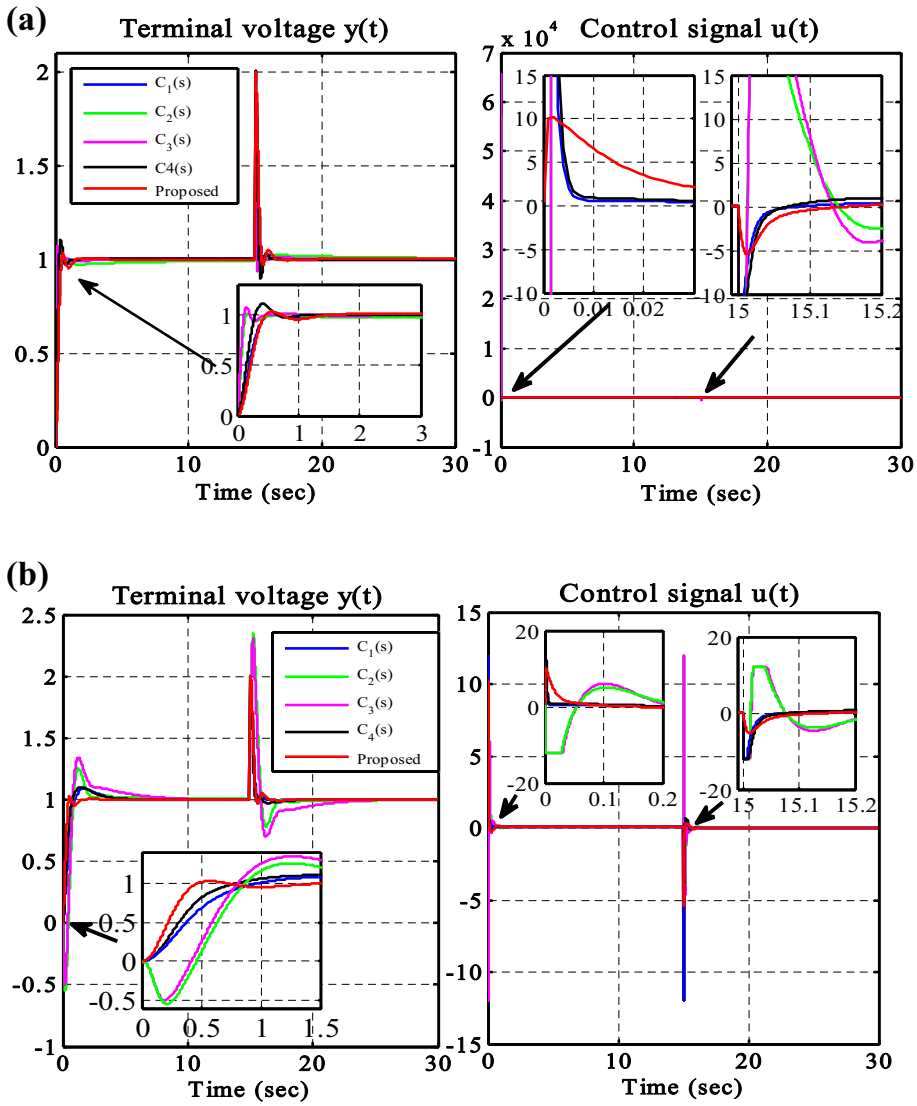

Fig. 14 Comparison of time response of the five controllers given in Table 4

The controller obtained using the proposed tuning method with the desired closed-loop transfer function is given by:

$$C_{\mathrm{p}}(s) = 0.0425 + \frac{0.0260}{s^{0.9802}} + 0.0308\ s^{0.7710} \tag{32}$$

The proposed controller will be compared with the robust H_{ω}-based controller proposed in [37] where its transfer function is given as:

$$K(s) = \frac{0.02883\ s^5 + 8156.28\, s^4 + 703621\ \mathrm{s}^3 + 15750024.5\ \mathrm{s}^2 + 48471744\ \mathrm{s} + 33417184.4}{\mathrm{s}^6 + 222.7\ \mathrm{s}^5 + 22584\ \mathrm{s}^4 + 1372617\ \mathrm{s}^3 + 53520000\ \ \mathrm{s}^2 + 1263200000\ \mathrm{s}} \tag{33}$$

Two controllers given by (32) and (33) are tested for five different cases for plant's parameters, where these cases involve nominal, minimum and maximum values of uncertain parameters.

Table 5 and Fig. 15 show comparison results of the two controllers (32) and (33) for five different cases of AVR system parameters where the two controllers satisfied a steady-state error $Ess = 0$ and $u_{max} = 0.7450$ with proposed controller and $u_{\max} = 0.7046$ for (33) in all five cases.

Figure 15 shows the time response for set-point tracking at $t = 0$ s and disturbance rejection at $t = 5$ s for the three first cases and 15 s for the last two cases. The control signals are also shown for two controllers (32) and (33) in the five cases presented in Table 5.

It can be noted that the proposed controller satisfies good performance and robustness as the robust controller (33).

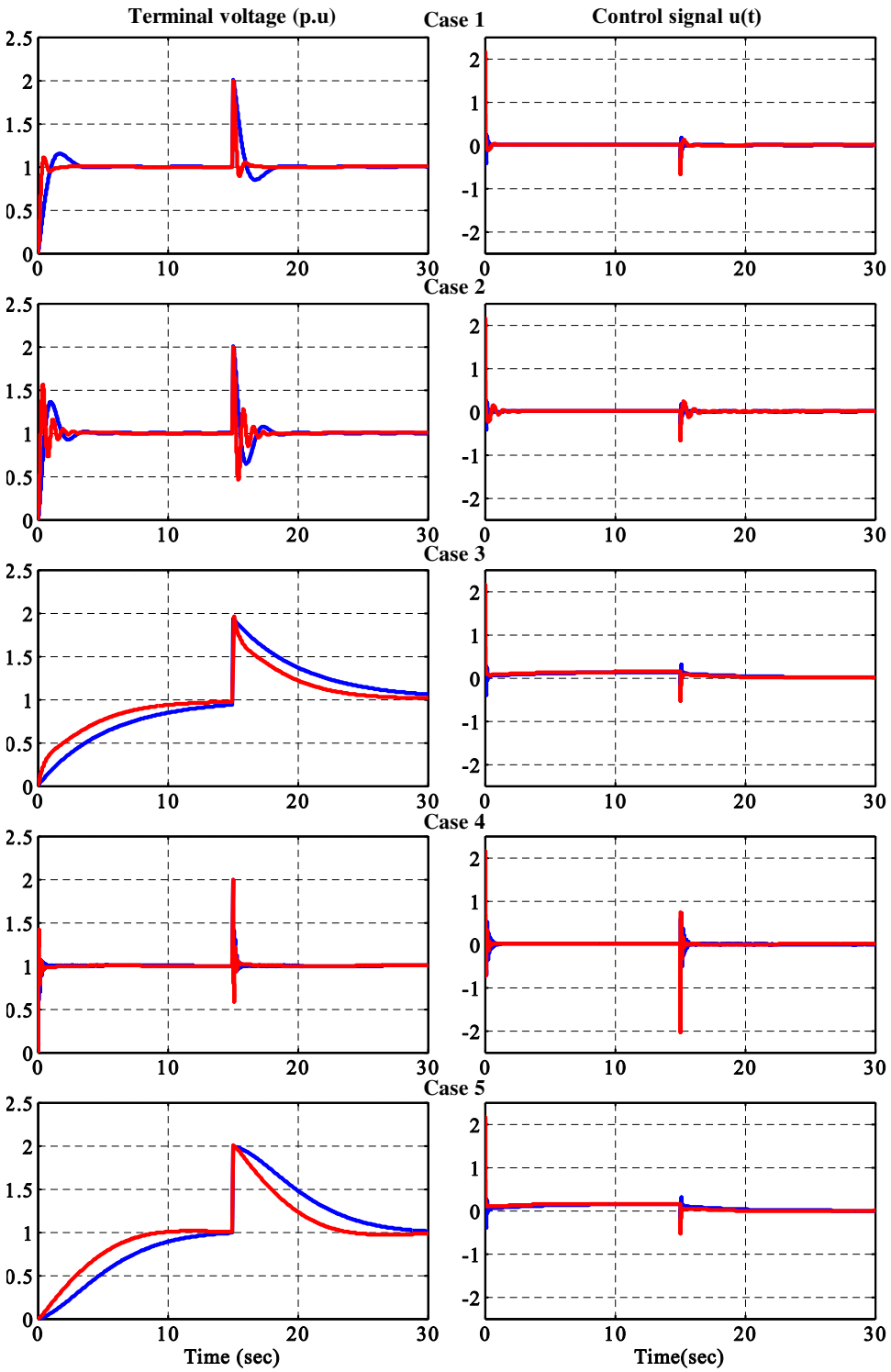

Fig. 15 Comparison of time response of the two controllers (32) red line and (33) blue line

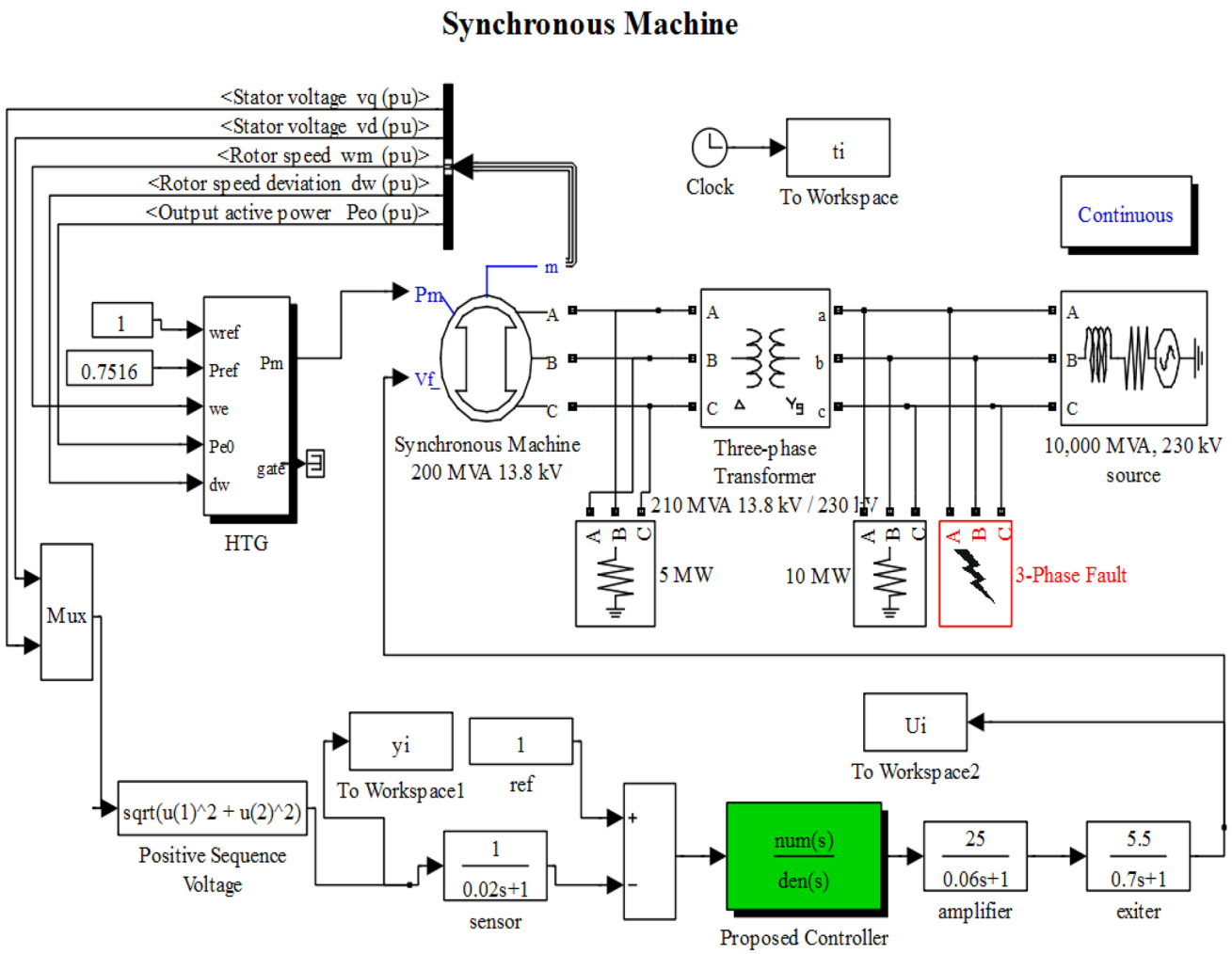

Fig. 16 The synchronous machine associated with the hydraulic turbine and governor (HTG) and excitation system (AVR) [38]

From these results, the proposed controller can be used in different operating conditions, which shows its robustness to the plant parameters variation.

4.3 Simulation of a real synchronous generator connected to a 230 kV network

Figure 16 shows the simulation of synchronous generator of 200 MVA, 13.8 kV [38]. The generator supplies the grid with 150MVA and at $t = 30.1$ s a three phases short circuit fault is simulated on the transformer bus for 6 cycle. After the fault is cleared, the terminal voltage output reach its desired value as shown in Fig. 17 where three controllers are compared namely: proposed controller, H_∞ controller and standard IEEE controller.

Figures 17 and 18 show the time response and controller output for system described in Fig. 16 by the three compared controller. Although the proposed controller and the robust Hinf controller have not been designed exactly for the

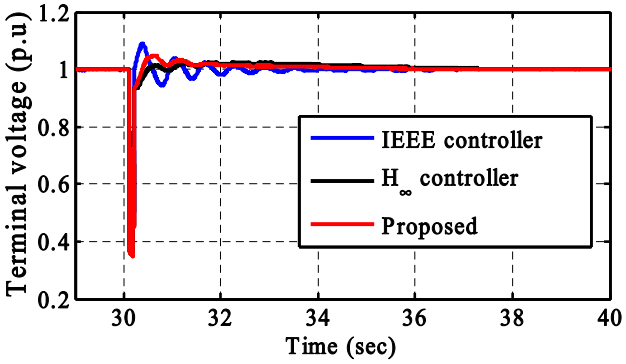

Fig. 17 The terminal voltage of the synchronous machine in 230 kV networks

used model of generator in [38], their performances are of good quality compared with the conventional IEEE controller which gives a saturated control law as shown in Fig. 18. The good performances obtained when using the controllers (32) and (33) are due to the robust design of H_∞ controller and

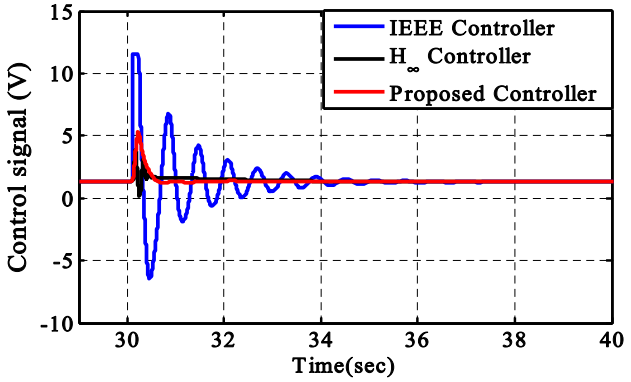

Fig. 18 Excitation voltage of the synchronous machine in 230 kV networks

the appropriate choice of the desired transfer function (31) in the proposed design methodology.

5 Conclusion

A novel fractional-order PID controller tuning method is proposed, where the controller is synthesized such that the closed-loop system behaves as Bode's ideal loop transfer function. The advantage of this tuning method is that it does not need the plant's model for controller design. In addition, the five parameters of $PI^{\lambda}D^{\mu}$ are semi-analytically derived which makes the proposed technique very useful for online implementation where the controller parameters are calculated from the plant's input–output data allowing the improvement of existing control. The simulation results have shown the efficiency of the proposed method for a class of high-order and time delay systems and confirm that the closed-loop systems with the proposed controller have the iso-damping property. In addition, present work illustrates that it can avoid difficulty to adjust the two parameters λ and μ where their values are known in the range [0 2] by the simple scanning of their discrete values and the control problem is solved without limitation of the five DOF of the $PI^{\lambda}D^{\mu}$ controller.

The additional contribution of this work is that we can use a delay-free-system as a desired closed-loop system for controlling a time delay system unlike the work presented in [24] that used the Bode's ideal integrator with time delay as reference open-loop model.

The application of the $PI^{\lambda}D^{\mu}$ controller to the AVR system shows the utility and efficiency of the proposed controller design methodology.

Author Contributions The first author has carried out all the research work in this manuscript.

Funding No funding is applicable.

Data availability Not applicable.

Code availability Not applicable.

Declarations

Conflict of interest Author has no competing interest.

References

1. Bode HW (1945) Network analysis and feedback amplifier design. D. Van Nostrand Co., New York
2. Åström KJ (2000) Limitations on control system performance. Eur J Control 6(1):2–20
3. Oustaloup A (1991) La commande CRONE: commande robuste d'ordre non entier. Hermes Science Publications, Paris
4. Podlubny I (1999) Fractional-order systems and $PI^{\lambda}D^{\mu}$ controllers. IEEE Trans Autom Control 44(1):208–214
5. Shah P, Agashe S (2016) Review of fractional PID controller. Mechatronics 38:29–41
6. Valério D, Da Costa JS (2006) Tuning of fractional PID controllers with Ziegler–Nichols-type rules. Signal Process 86(10):2771–2784
7. Monje CA et al (2008) Tuning and auto-tuning of fractional order controllers for industry applications. Control Eng Pract 16(7):798–812
8. Li H, Luo Y, Chen Y (2009) A fractional order proportional and derivative (FOPD) motion controller: tuning rule and experiments. IEEE Trans Control Syst Technol 18(2):516–520
9. Luo Y, Chen Y (2009) Fractional order [proportional derivative] controller for a class of fractional order systems. Automatica 45(10):2446–2450
10. Luo Y et al (2010) Tuning fractional order proportional integral controllers for fractional order systems. J Process Control 20(7):823–831
11. Tavakoli-Kakhki M, Haeri M (2011) Fractional order model reduction approach based on retention of the dominant dynamics: application in IMC based tuning of FOPI and FOPID controllers. ISA Trans 50(3):432–442
12. Vu TNL, Lee M (2013) Analytical design of fractional-order proportional-integral controllers for time-delay processes. ISA Trans 52(5):583–591
13. Bettayeb M, Mansouri R (2014) Fractional IMC-PID-filter controllers design for non integer order systems. J Process Control 24(4):261–271
14. Saidi B et al (2015) Bode shaping-based design methods of a fractional order PID controller for uncertain systems. Nonlinear Dyn 80(4):1817–1838
15. Fergani N, Charef A (2016) Process step response based fractional $PI^{\lambda}D^{\mu}$ controller parameters tuning for desired closed loop response. Int J Syst Sci 47(3):521–532
16. Keziz B, Djouambi A, Ladaci S (2020) A new fractional order controller tuning method based on Bode's ideal transfer function. Int J Dyn Control 8(3):932–942
17. Saxena S, Hote YV (2022) Design of robust fractional-order controller using the Bode ideal transfer function approach in IMC paradigm. Nonlinear Dyn 107(1):983–1001
18. Muresan CI, De Keyser R (2022) Revisiting ziegler-Nichols. A fractional order approach. ISA Trans 20:22. https://doi.org/10.1016/j.isatra.2022.01.017
19. Biswal SS, Swain DR, Rout PK (2022) Inter-area and intra-area oscillation damping for UPFC in a multi-machine power system based on tuned fractional PI controllers. Int J Dyn Control. https://doi.org/10.1007/s40435-021-00891-4

20. Rivera DE, Morari M, Skogestad S (1986) Internal model control: PID controller design. Ind Eng Chem Process Des Dev 25(1):252–265
21. Chen D, Seborg DE (2002) PI/PID controller design based on direct synthesis and disturbance rejection. Ind Eng Chem Res 41(19):4807–4822
22. Jeng J-C (2015) A model-free direct synthesis method for PI/PID controller design based on disturbance rejection. Chemom Intell Lab Syst 147:14–29
23. Barbosa RS, Silva MF, Machado JT (2009) Tuning and application of integer and fractional order PID controllers. In: Tenreiro Machado JA (ed) Intelligent engineering systems and computational cybernetics. Springer, Dordrecht, pp 245–255
24. Yumuk E, Güzelkaya M, Eksin İ (2019) Analytical fractional PID controller design based on Bode's ideal transfer function plus time delay. ISA Trans 91:196–206
25. Bettayeb M et al (2017) Smith predictor based fractional-order-filter PID controllers design for long time delay systems. Asian J Control 19(2):587–598
26. Feliu-Batlle V et al (2009) Smith predictor based robust fractional order control: Application to water distribution in a main irrigation canal pool. J Process Control 19(3):506–519
27. Bouyedda H et al (2019) Identification and control design for a class of non-minimum phase dead-time systems based on fractional-order smith predictor and genetic algorithm technique. Int J Dyn Control 7(3):914–925
28. Vavilala SK, Thirumavalavan V (2021) Tuning of the two degrees of freedom FOIMC based on the Smith predictor. Int J Dyn Control 9(3):1303–1315
29. Laifa S, Boudjehem B, Gasmi H (2021) Direct synthesis approach to design fractional PID controller for SISO and MIMO systems based on Smith predictor structure applied for time-delay non integer-order models. Int J Dyn Control. https://doi.org/10.1007/s40435-021-00831-2
30. Chen Y, Moore KL (2005) Relay feedback tuning of robust PID controllers with iso-damping property. IEEE Trans Syst Man Cybernet Part B (Cybernetics) 35(1):23–31
31. Bouakkaz MS et al (2020) Dynamic performance evaluation and improvement of PV energy generation systems using Moth Flame Optimization with combined fractional order PID and sliding mode controller. Sol Energy 199:411–424
32. Frikh ML et al (2021) Fractional order PID controller design for wind turbine systems using analytical and computational tuning approaches. Comput Electr Eng 95:107410
33. Bingul Z, Karahan O (2018) A novel performance criterion approach to optimum design of PID controller using cuckoo search algorithm for AVR system. J Franklin Inst 355(13):5534–5559
34. Köse E (2020) Optimal control of AVR system with tree seed algorithm-based PID controller. IEEE Access 8:89457–89467
35. Sikander A et al (2018) A novel technique to design cuckoo search based FOPID controller for AVR in power systems. Comput Electr Eng 70:261–274
36. Zeng G-Q et al (2015) Design of fractional order PID controller for automatic regulator voltage system based on multi-objective extremal optimization. Neurocomputing 160:173–184
37. Modabbernia M et al (2020) Robust control of automatic voltage regulator (AVR) with real structured parametric uncertainties based on H_∞ and μ-analysis. ISA Trans 100:46–62
38. Mathworks (2019) Model hydraulic turbine and proportional–integral–derivative (PID) governor system—Simulink. https://nl.mathworks.com/help/physmod/sps/examples/synchronous-machine.html.